Neuro-Oncology

22(7), 967–978, 2020 | doi:10.1093/neuonc/noaa029 | Advance Access date 21 February 2020

The role of extracellular vesicles and PD-L1 in glioblastoma-mediated immunosuppressive monocyte induction

Benjamin T. Himes, Timothy E. Peterson, Tristan de Mooij, Luz M. Cumba Garcia, Mi-Yeon Jung, Sarah Uhm, David Yan, Jasmine Tyson, Helen J. Jin-Lee, Daniel Parney, Yasmina Abukhadra, Michael P. Gustafson, Allan B. Dietz, Aaron J. Johnson, Haidong Dong, Rachel L. Maus, Svetomir Markovic, Fabrice Lucien, and Ian F. Parney

Department of Neurologic Surgery (B.T.H., T.E.P., T.D.M., M-Y.J., S.U., D.Y., J.T., H.J.J-L., D.P., Y.A., I.F.P.), Department of Immunology (B.T.H., L.M.C.G., A.B.D., A.J.J., H.D., R.L.M., S.M., I.F.P.), Graduate School of Biomedical Sciences (L.M.C.G.), Department of Lab Medicine and Pathology (M.P.G., A.B.D.), Department of Oncology (R.L.M., S.M.), and Department of Urology (H.D., F.L.), Mayo Clinic, Rochester, Minnesota

Corresponding Author: Dr. Ian F. Parney MD, PhD, Mayo Clinic, 200 First Street SW, Rochester, MN, USA, 55905 (parney.ian@mayo.edu).

Abstract

Background. Immunosuppression in glioblastoma (GBM) is an obstacle to effective immunotherapy. GBM-derived immunosuppressive monocytes are central to this. Programmed cell death ligand 1 (PD-L1) is an immune checkpoint molecule, expressed by GBM cells and GBM extracellular vesicles (EVs). We sought to determine the role of EV-associated PD-L1 in the formation of immunosuppressive monocytes.

Methods. Monocytes collected from healthy donors were conditioned with GBM-derived EVs to induce the formation of immunosuppressive monocytes, which were quantified via flow cytometry. Donor-matched T cells were subsequently co-cultured with EV-conditioned monocytes in order to assess effects on T-cell proliferation. PD-L1 *constitutive* overexpression or short hairpin RNA–mediated knockdown was used to determined the role of altered PD-L1 expression.

Results. GBM EVs interact with both T cells and monocytes but do not directly inhibit T-cell activation. However, GBM EVs induce immunosuppressive monocytes, including myeloid-derived suppressor cells (MDSCs) and nonclassical monocytes (NCMs). MDSCs and NCMs inhibit T-cell proliferation in vitro and are found within GBM in situ. EV PD-L1 expression induces NCMs but not MDSCs, and does not affect EV-conditioned monocytes T-cell inhibition.

Conclusion. These findings indicate that GBM EV-mediated immunosuppression occurs through induction of immunosuppressive monocytes rather than direct T-cell inhibition and that, while PD-L1 expression is important for the induction of specific immunosuppressive monocyte populations, immunosuppressive signaling mechanisms through EVs are complex and not limited to PD-L1.

Key Points

1. Glioblastoma-derived extracellular vesicles generate immunosuppressive monocytes.
2. PD-L1 expression on tumor-derived EVs is important for the formation of nonclassical monocytes.
3. Tumor-derived EVs may be a critical mechanism of immunosuppression in GBM.

Importance of the Study

Immunotherapy has revolutionized the treatment of some cancers but has failed to yield similar results in GBM. GBM patients exhibit profound immunosuppression, which may explain these failures, but the underlying immunosuppressive mechanisms remain poorly understood. We describe the induction of immunosuppressive monocytes by GBM-derived EVs, which may be a primary pathway of immunosuppression in GBM. Further, we demonstrate that the immunomodulatory protein PD-L1 is important for the induction of NCMs, but not MDSCs, underscoring the multifactorial signaling role of EVs and the complexity of tumor-mediated immunosuppression.

Glioblastoma (GBM) is the most common and deadly primary brain tumor, with a median survival of just over 14 months in spite of maximal treatment.[1,2] The current standard of care includes surgical resection, followed by temozolomide chemotherapy and fractionated radiotherapy.[1,3] There is an urgent need to develop novel therapies, and immunotherapies hold significant promise. These treatments range from immunologic "checkpoint" inhibitors that energize the antitumor activity of the immune system, to chimeric antigen receptor (CAR) T cells that target specific tumor antigens.[4,5] The interaction between programmed cell death ligand 1 (PD-L1) and its receptor programmed cell death 1 (PD-1) has been of particular interest. PD-L1 is expressed by GBM, and PD-1/PD-L1 interactions are implicated in T-cell exhaustion and curbing the immune response.[6] Inhibition of this axis has shown promise in the treatment of several cancers, with antibody therapies directed toward both PD-1 and PD-L1 in clinical use.[7–9]

The efficacy of such therapies for GBM is limited by the profound immunosuppression exhibited in GBM patients.[10] GBM patients have demonstrated substantial reductions in circulating cluster of differentiation (CD)4+ T cells.[11–13] The mechanisms of this immunosuppression are not completely characterized, but tumor-mediated induction of myeloid-derived suppressor cells (MDSCs) plays an important role.[14–17] These cells exert both local and systemic immunosuppressive effects via the release of immunomodulatory cytokines and inhibition of T-cell proliferation.[18,19] More recently, nonclassical monocytes (NCMs), exhibiting some properties of type 2 macrophages, have been described, and may also contribute to tumor-mediated immunosuppression.[18,20–22] These CD14+CD16+ monocytes may take on an immunosuppressive phenotype when they also express PD-1, as has been seen in immune dysfunction in sepsis and chronic infection.[23,24] Nonclassical monocytes are often described as "patrolling" monocytes and have been implicated in the antitumor immune response, and so increasing PD-1 expression in these cells may imply impaired antitumor immunity.[25] These immunosuppressive monocytes have been described both in the tumor microenvironment and systemically in patients with cancer, including GBM.[18,21] However, the mechanisms by which they mediate immunosuppression are poorly understood. They may locally release immunomodulatory cytokines or alter amino acid metabolism, but such mediators do not reach sufficient quantities in systemic circulation to explain the profound immunosuppression seen in patients.[13,15,16]

Extracellular vesicles (EVs) are one mechanism by which GBM may exert immunosuppressive effects. EVs chiefly comprise small (<100 nm) exosomes and larger (100–1000 nm) microvesicles.[26,27] EVs are a critical means of cell-cell communication, shed by both normal cells and tumors, including GBM.[28,29] EVs can carry proteins and small RNAs that transmit an array of signals to target cells, including PD-L1.[6,29] Recent data have suggested that GBM-derived EVs directly inhibit T cells through PD-L1/PD-1 interactions.[6] Additionally, tumor-derived EVs have been implicated in the induction of MDSCs in other cancers.[30] We sought to interrogate the role of EVs and PD-L1 expression as potential mechanisms for tumor-mediated immunosuppression. We found that GBM-derived EVs did not appreciably inhibit T cells directly regardless of PD-L1 expression, but rather found that these EVs induce the formation of immunosuppressive monocytes. Further, we found that while PD-L1 expression was not vital to the induction of traditional MDSCs, the expression of PD-L1 in GBM-derived EVs induced the formation of PD-1 expressing nonclassical monocytes.

Materials and Methods

GBM Cell Culture

GBM tissue was obtained during surgery at the Mayo Clinic in Rochester, Minnesota. Specimens were obtained with written, informed consent following approval by the Mayo Clinic Institutional Review Board (IRB#12-003458). Cell suspensions were generated by passing tissue through a 40 μm mesh and grown as neurospheres in serum-free media with epidermal growth factor, basic fibroblast growth factor, and N2 supplement as previously described.[31] Neurospheres were transferred to DMEM:F12 media with 1% penicillin/streptomycin and 10% fetal calf serum to generate differentiated-adherent cell lines. To generate a PD-L1 overexpression cell line, the wild-type (WT) primary dBT116 cell line (dBT116 WT) was transduced with a lentivirus encoding human PD-L1 driven by a cytomegalovirus promotor (Applied Biological Materials). To generate a PD-L1 knockdown cell line, the wild-type dBT116 cell line was transduced with a lentivirus encoding human short hairpin (sh)RNA against PD-L1 driven by an H1 promoter (Santa Cruz Biotechnology). Both the PD-L1 overexpressing (OX) cells (dBT116 PD-L1 OX) and PD-L1 knockdown (KD) cells (dBT116 PD-L1 KD) were grown in

selection media containing puromycin (2 μg/mL). All cultures were maintained at 37°C, 5% CO_2.

Extracellular Vesicle Harvesting

Collection of EVs from undifferentiated (uBT) cell lines was by centrifugation of serum-free culture media at 3000 rpm for 10 minutes to remove any cellular debris. Supernatant was subsequently centrifuged for 16 hours at 24 000 rpm to concentrate EVs. The 200–500 μL EV-enriched fraction was used for subsequent studies. EV concentration was determined by quantification of total protein via bicinchoninic acid assay (Pierce/Thermo Fisher). Harvesting of differentiated (dBT) cell line-derived EVs proceeded in similar fashion, but media was first switched from 10% DMEM:F12 to serum-free media for 72 h prior to centrifugation.

NanoSight Analysis of Extracellular Vesicles

Cells were maintained in serum-free media for 72 hours. Extracellular vesicles were then directly analyzed from the conditioned media for size and concentration using a NanoSight 300 particle analyzer (Malvern Panalytical). Extracellular vesicles were diluted 1:100 in water, and 3- to 30-second movies were analyzed and averaged for each cell line.

PD-L1 ELISA

Enzyme-linked immunosorbent assay (ELISA) was performed as previously described.[32] Briefly, 2 mouse immunoglobulin G1 anti–PD-L1 monoclonal antibodies (2.2B and 5H1-A3) that bind different extracellular regions of PD-L1 were validated and used for this assay. High-binding polystyrene plates (Corning Life Sciences) were coated for 2 hours at room temperature with 0.2 μg/well of capture antibody 2.2B. After washing, wells were blocked using Superblock (Pierce/Thermo Fisher). Standards and isolated EVs were added in duplicates and incubated overnight at 4°C. Biotinylated 5H1-A3 detection antibody was added and incubated for 1 hour followed by addition of horseradish peroxidase–conjugated streptavidin (BD Biosciences). Plates were developed with TMB (3,3′,5,5′-tetramethylbenzidine; Pierce), and the reaction stopped using 0.5 N H_2SO_4 and read at 450 nm using a Benchmark Plus plate reader (Bio-Rad). For calibration, each plate was loaded with duplicate parallel dilutions of recombinant B7-H1 fusion protein (R&D Systems) ranging in concentration from 0.01 to 20 ng/mL.

Monocyte and T-Cell Isolation

Healthy blood donors were used as a source of peripheral blood mononuclear cells (PBMCs).[33] PBMCs were isolated via Ficoll gradient centrifugation. Monocytes and T cells were isolated via magnetic bead separation for CD14+ and CD3+ cells, respectively (Miltenyi Biotec). T cells were maintained in suspension in 10% fetal bovine serum RPMI (Roswell Park Memorial Institute) media with L-glutamine until initiation of co-culture experiments with monocytes.

Immunofluorescence

EVs were labeled with PKH27 according to the manufacturer's protocol and incubated with normal human monocytes in a 96-well plate for 24 hours. Monocytes were then fixed with 2% paraformaldehyde for 15 minutes and blocked with 10% normal goat serum for 30 minutes. Slides were incubated for 1 hour with anti–PD-1 (Cell Signaling, clone E1L3N, rabbit monoclonal) followed by rabbit anti-mouse CY5 secondary antibody (Jackson ImmunoResearch Labs) for 45 minutes. Nuclei were stained with 10 μg/mL Hoechst 33258 (Sigma-Aldrich).

Flow Cytometry

In all cases, cells were harvested and washed with phosphate buffered saline (PBS) and fluorescence activated cell sorting (FACS) buffer (1.8% bovine serum albumin, 1 mm EDTA in PBS) prior to staining. Cells were resuspended in 100 μL FACS buffer, and 3 μL of each fluorochrome was added (1 μL in the case for viability dye Ghost 780, Tonbo Biosciences) and incubated for 30 minutes. Cells were subsequently washed with FACS buffer and fixed with 2% paraformaldehyde prior to flow cytometry. All flow cytometry experiments were carried out using an LSRII flow cytometer (Becton Dickinson) and all subsequent data analysis was performed using FlowJo version 10.

Western Blotting

All western blots were carried out on 10–20% sodium dodecyl sulfate–polyacrylamide gel electrophoresis gel (Bio-Rad) and transferred onto polyvinylidene difluoride membrane. All membranes were blocked in 5% milk in Tris-buffered 0.1% Tween 20. Primary antibodies used included overnight incubation at 4°C with PD-L1 (Cell Signaling, clone E1L3N, rabbit monoclonal), CD63 (Santa Cruz Biotechnology, clone MX-49.129.5, mouse monoclonal), CD9 (Cell Signaling Technology, clone D8O1A, rabbit monoclonal), HSP-90 (Cell Signaling, #4874, rabbit polyclonal), α-tubulin (Sigma-Aldrich, clone DM1A, mouse monoclonal). Secondary antibody was horseradish peroxidase–conjugated goat anti-rabbit or goat anti-mouse (Jackson ImmunoResearch) as appropriate. Membranes were developed using SuperSignal Pico PLUS Chemiluminescent substrate (Pierce/Thermo Fisher).

Sample Preparation for Nanoscale Flow Cytometry

Mixed were 1.8 mL of MACSflex microbeads (Miltenyi Biotec) with 200 μL biomolecule-mixture composed of 170 μL of 50 mM MES (2-(N-morpholino)ethanesulfonic acid) buffer (900 μL of water and 100 μL of MES buffer), and 30 μL of PD-L1 antibody (BioLegend). Samples were incubated for 2 hours at room temperature followed by overnight at 4°C. The homogenized solution was transferred to μMACS Separator columns and several washes were performed, followed by elution of PD-L1 conjugated microbeads with MACSflex Storage Buffer per the

manufacturer's (Miltenyi Biotec) protocol. Twenty microliters of the eluted PD-L1–conjugated microbeads were mixed with 40 μL of PD-L1 overexpressed EVs (derived from dBT116 PD-L1 OX cell line) isolated by ultracentrifugation, and 60 μL of MACS buffer. Samples were incubated for 1 hour and the homogenized solution was transferred to the μMACS Separator as above. We then collected the PD-L1– (from wash) fraction. The PD-L1+ (eluted) fraction was obtained by eluting the column with a 100 μL of MACSflex Storage Buffer. Nanoscale flow cytometry analysis was performed in both fractions (washes and eluted).

Nanoscale Flow Cytometry

PD-L1– (wash fraction) and PD-L1+ (eluted fraction) EVs were analyzed using the A60-Micro Plus nanoscale flow cytometer (Apogee FlowSystems). Sample flow rate was set at 1.5 μL/min for all measurements and the time of acquisition was held constant for all samples at 60 seconds. Before sample analysis, A60-Micro Plus was calibrated using a reference bead mix as previously described.[34] Briefly, polystyrene and silica beads with diameters ranging from 100 nm to 1300 nm were used to evaluate A60-Micro sensitivity for light-scatter detection. Light-scatter triggering thresholds were set such that all events between 100 nm and 1000 nm were gated as EVs. Data were analyzed using FlowJo v10.5 software.

MDSC Induction

CD14+ monocytes were plated at 10^5 cells/well in flat-bottomed 96-well plates. EVs were added at 20 μg/well in a total volume of 200 μL serum-free media. Monocytes were conditioned with EVs for 72 hours at 37 °C in hypoxic conditions (1% O_2) in order to induce MDSC formation. Following 72 hours of MDSC induction monocytes were harvested, stained, and fixed for flow cytometry.

T-Cell Proliferation

T cells were stained with CellTrace CFSE (carboxyfluorescein succinimidyl ester; Thermo Fisher) in accordance with the manufacturer's instructions. Stimulated T cells were plated at 10^5 cells per well with αCD3/αCD28 DynaBeads (Thermo Fisher) in a 1:1 ratio in the presence of either 20μg EVs or EV-conditioned monocytes at 37°C at 5% CO_2 for 5 days. CFSE dilution was assessed by flow cytometry. For monocyte co-culture experiments, T cells were added to monocytes in a 1:1 ratio.

Statistics

All statistical analysis was performed in GraphPad Prism 8 software. In all MDSC and NCM induction studies, one-way ANOVA was performed, with subsequent Dunnett multiple comparisons test, utilizing unconditioned monocytes as the single reference group. All T-cell co-culture studies were conducted in pairwise fashion to account for the addition of donor-matched T cells, and so a repeated measures ANOVA was employed with subsequent Dunnett multiple comparisons test with the unconditioned co-culture as the reference group. (Throughout this manuscript: $*P < 0.05$, $**P \leq 0.01$, $***P \leq 0.001$, and $****P < 0.0001$.)

Results

Glioblastoma Cells Release PD-L1+ EVs

We cultured human GBM cells in both serum-exposed differentiated monolayer (dBT cell lines) and serum-free undifferentiated spheroid (uBT) systems, the latter of which has been shown to enrich for stemlike tumor cells (Fig. 1A).[31] Both uBT and dBT cell lines express the stemlike markers Sox2 (sex determining region Y–box 2) and nestin but only dBT cell lines express the mature glial-neuronal markers glial fibrillary acidic protein (GFAP) and β-tubulin (Fig. 1B). When cultured for 72 hours in serum-free conditions, and following removal of cellular debris, both dBT and uBT cell lines produce abundant extracellular vesicles predominantly 100–400 nm in size, which remained consistent across cell lines (Fig. 1C). In addition to expressing known EV-associated proteins (CD63, CD9, HSP90), multiple dBT cell lines express PD-L1 in both EVs and whole-cell lysates, but in uBT cell lines PD-L1 expression was predominantly detected in the EVs with minimal levels in whole-cell lysate (Fig. 1D). This remained the case even following treatment with 72 hours of interferon-γ (Supplementary Figure 1), which has been implicated in the induction of immunosuppressive PD-L1 expression.[35] Soluble PD-L1 ELISA assay detected increased soluble PD-L1 in EV-enriched media following ultracentrifugation (Fig. 1E). In the dBT116 cell line, we developed constitutive PD-L1 OX and shRNA-mediated KD variants, and confirmed change in PD-L1 expression via flow cytometry and western blot (Fig. 1F; Supplementary Figure 2). Changes in PD-L1 expression did not impact the overall shedding of EVs from these altered dBT116 cell lines, though there was a mild trend toward increased release of larger EVs (>100 nm) by PD-L1 OX cells (Supplementary Figure 2A). Expression of EV-associated proteins CD9 and CD63 was not altered with changes in PD-L1 expression (Fig. 1F). Confocal microscopy showed PD-L1 expression in glioma cell membrane blebs compatible with microvesicle (larger EV) release and demonstrated PD-L1, particularly in larger GBM EVs (Fig. 1G). Nanoscale flow cytometry further confirmed the presence of PD-L1+ GBM EVs predominantly >100 nm and demonstrated that these could be enriched by magnetic bead separation for PD-L1 (Fig. 1H). Together, these findings demonstrate PD-L1 expression in the extracellular vesicles of both differentiated and stemlike human GBM cell cultures, that this occurs mostly in EVs >100 nm, and that altered PD-L1 expression in GBM cells results in a concomitant change in EV-associated shed PD-L1 expression.

T Cells Are Not Inhibited Directly by GBM-Derived EVs

The ability of GBM-derived EVs to directly inhibit T-cell proliferation in a PD-L1–dependent fashion has been recently

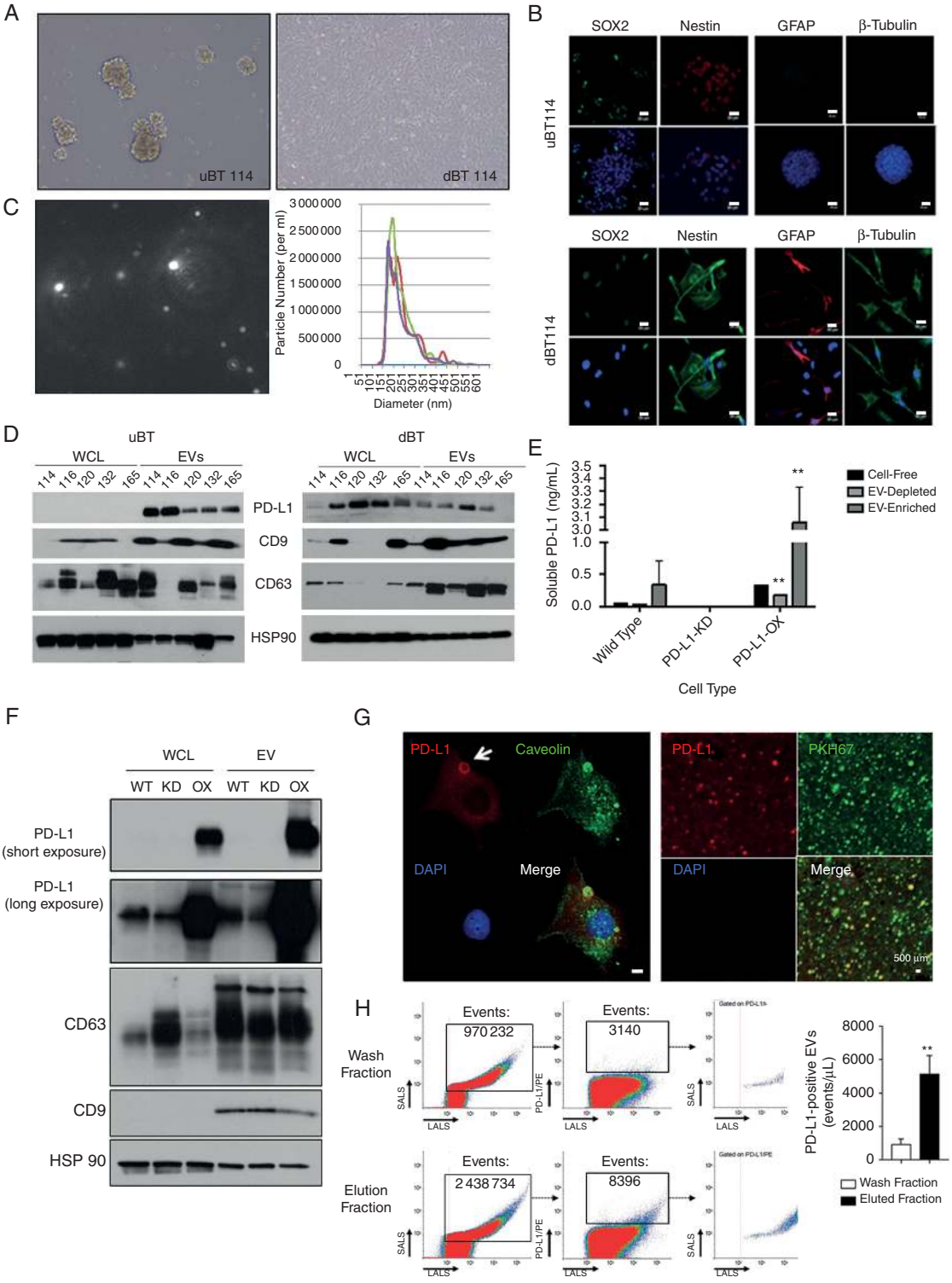

Fig. 1 Stemlike and differentiated glioblastoma cells release PD-L1+ EVs. (A) Low power light microscopy images of undifferentiated (uBT, left) and differentiated (dBT, right) cell lines in culture, in serum-free and serum-containing growth conditions, respectively. (B) Representative confocal microscopy images of uBT (top) or dBT (bottom) cells demonstrating expression of Sox2, nestin, GFAP, or β-tubulin alone (top rows) or merged with DAPI (4′,6′-diamidino-2-phenylindole) staining (bottom rows). Scale bars, 20 µm. (C) EVs in GBM culture media as visualized by the NanoSight nanotracker system, left panel with representative histogram of nanoparticle size in PD-L1 WT (blue), overexpressed (yellow), and knockdown (red). (D) Western blot of whole cell lysate (WCL) and EV for PD-L1, caveolin-1, CD9, CD63, and HSP-90 for uBT (left) and dBT (right) cell lines. (E) ELISA quantification of soluble PD-L1 in media derived from dBT116 cells, in EV-enriched or depleted fractions as indicated,

reported.[6] We found that both GBM cells (Fig. 2A) and GBM-derived EVs (Fig. 2B) associate with T cells in vitro at least in part via PD-1/PD-L1 colocalization. However, upon αCD3/αCD28 stimulation, we did not observe significant reduction in T-cell proliferation following CFSE staining and 5 days of culture with 20 μg of either uBT- or dBT-derived EVs (Fig. 2C, D). In order to determine the effect of EV PD-L1 expression on T-cell proliferation, we co-cultured EVs derived from dBT116 cell lines constitutively overexpressing PD-L1 or with shRNA-mediated PD-L1 knockdown with CFSE-labeled T cells activated via αCD3/αCD28 stimulation. No difference in T-cell proliferation was observed (Fig. 2E). This observation could not be explained by increased cell death as measured by propidium iodide/annexin V staining (Fig. 2F). We also investigated the role of differential PD-L1 expression on the induction of regulatory T cells (Tregs) following co-culture of activated T cells with EVs and were unable to detect any differential Treg induction (Supplementary Figure 3).

GBM-Derived EVs Induce the Formation of Myeloid-Derived Suppressor Cells and PD-1+Nonclassical Monocytes

We have previously reported that supernatant from GBM cell culture induces the formation of MDSCs.[36] Because this supernatant includes EVs, we sought to interrogate the ability of GBM-derived EVs to induce MDSC formation by co-culturing EVs with healthy donor–derived CD14+ monocytes. In order to assess EV-monocyte association, EVs were labeled with PKH27 prior to co-culture with monocytes. EVs clearly associate with monocytes when cultured together in hypoxic conditions for 24 hours, and do this in proximity to PD-1 in monocytes when it is present (Fig. 3A). A minority of healthy donor monocytes express PD-1 at baseline, though the majority express CD80 (B7-1), a potential alternative ligand for PD-L1 (Supplementary Figure 4). In order to assess their impact on immunosuppressive monocyte formation, GBM EVs were co-cultured with donor monocytes in hypoxic conditions for 72 hours. Our group and others have previously described that hypoxia, a critical component of the tumor microenvironment, potentiates the induction of MDSCs.[36–38] Monocytes were subsequently examined by flow cytometry for the presence of monocytic MDSCs (CD14+/HLA-DR^{low}) or nonclassical monocytes (CD14+/PD-1+/CD16+/HLA-DR^{high}), following a CD11b+ parent gate.[13,16,22,39,40] Co-culture with uBT-derived EVs did not significantly increase in MDSC induction (Fig. 3B). However, uBT-derived EVs did increase induction of NCMs, though this trend reached statistical significance in only the case of uBT114-derived EVs (13.7% vs 59.8%, $P = 0.039$; Fig. 3D). With regard to the differentiated GBM cell lines, only dBT116 EVs induced the induction of MDSCs to a significant degree (28.6% in naïve vs 68% in EV-conditioned, $P = 0.0075$; Fig. 3C) but both dBT114 and dBT120-derived EVs significantly induced the formation of NCMs (46.2% and 36.7% in EV-conditioned vs 20.2% in untreated, $P = 0.0007$ and $P = 0.0177$, respectively; Fig. 3E). Neither uBT- nor dBT-derived EVs appreciably altered the proportion of CD14+ cells in co-culture, with the notable exception of dBT116 EVs, which resulted in a very high proportion of CD14+ cells following co-culture (Supplementary Figure 5). This finding may explain the apparent depression in NCM formation following dBT co-culture as a proportion of CD14+ cells (Fig. 3E). Taken together, these findings suggest that GBM-derived EVs can induce the formation of either nonclassical monocytes or MDSCs, but not necessarily both simultaneously. A portion of both MDSCs and NCMs demonstrated interleukin (IL)-10 expression (Supplementary Figure 6). Lastly, in freshly resected GBM tissue, we were able to identify both NCMs and MDSCs, providing a clinical correlate for this model (Supplementary Figure 7).

GBM-EV–Treated Monocytes Are Immunosuppressive

We next sought to assess the immunosuppressive function of monocytes induced by GBM-EV exposure. To that end, we treated monocytes with GBM-EVs and subsequently co-cultured these cells with donor-matched T cells labeled with CFSE stimulated with αCD3/αCD28 beads. Although there was significant variability from donor to donor, monocytes conditioned with both uBT and dBT EVs resulted in reduced T-cell proliferation relative to unconditioned monocytes (Fig. 4A–C). This effect was greater for dBT GBM-EV–conditioned monocytes than for uBT GBM-EV–conditioned cells, with absolute reductions in T-cell proliferation in all co-culture experiments, and significant reductions in proliferation following co-culture with dBT114 and dBT116 EV-conditioned monocytes (60.4% and 52.6% proliferation vs 77.5% proliferation in co-culture with unconditioned monocytes, $P = 0.015$ and $P = 0.031$, respectively).

PD-L1 Expression Is Important for the Induction of NCMs but Not MDSCs

Having demonstrated that GBM-EVs induce monocytes to differentiate into NCMs and MDSCs, that GBM-EV–conditioned monocytes inhibit T cells, and that the PD-L1/PD-1 axis appears to be associated with this interaction, we next sought to determine the importance of PD-L1 expression in the induction of MDSCs and NCMs. Using EVs derived from dBT116 cell lines overexpressing PD-L1 or with PD-L1 knockdown via shRNA (Fig. 1F), we assessed the induction

Fig. 1 Continued with the EV-enriched fraction comprising the EV-enriched "pellet" following ultracentrifugation and the EV-depleted fraction comprising the supernatant. (F) Western blot characterization of PD-L1 expression in WT, KD, and OX dBT116 cells. (G) Immunofluorescent staining of PD-L1 (red) caveolin (green) in a representative dBT cell, demonstrating a large EV expressing PD-L1 (left, scale bar 5 μm), and immunofluorescent staining for PD-L1 (red) or cell membrane (PKH67, green) in EVs (right, scale bar 500 nm). (H) Nanoscale flow cytometry with PD-L1 staining in EV depleted or enriched media (left panel), and quantification of PD-L1 gating shown in (right panel).

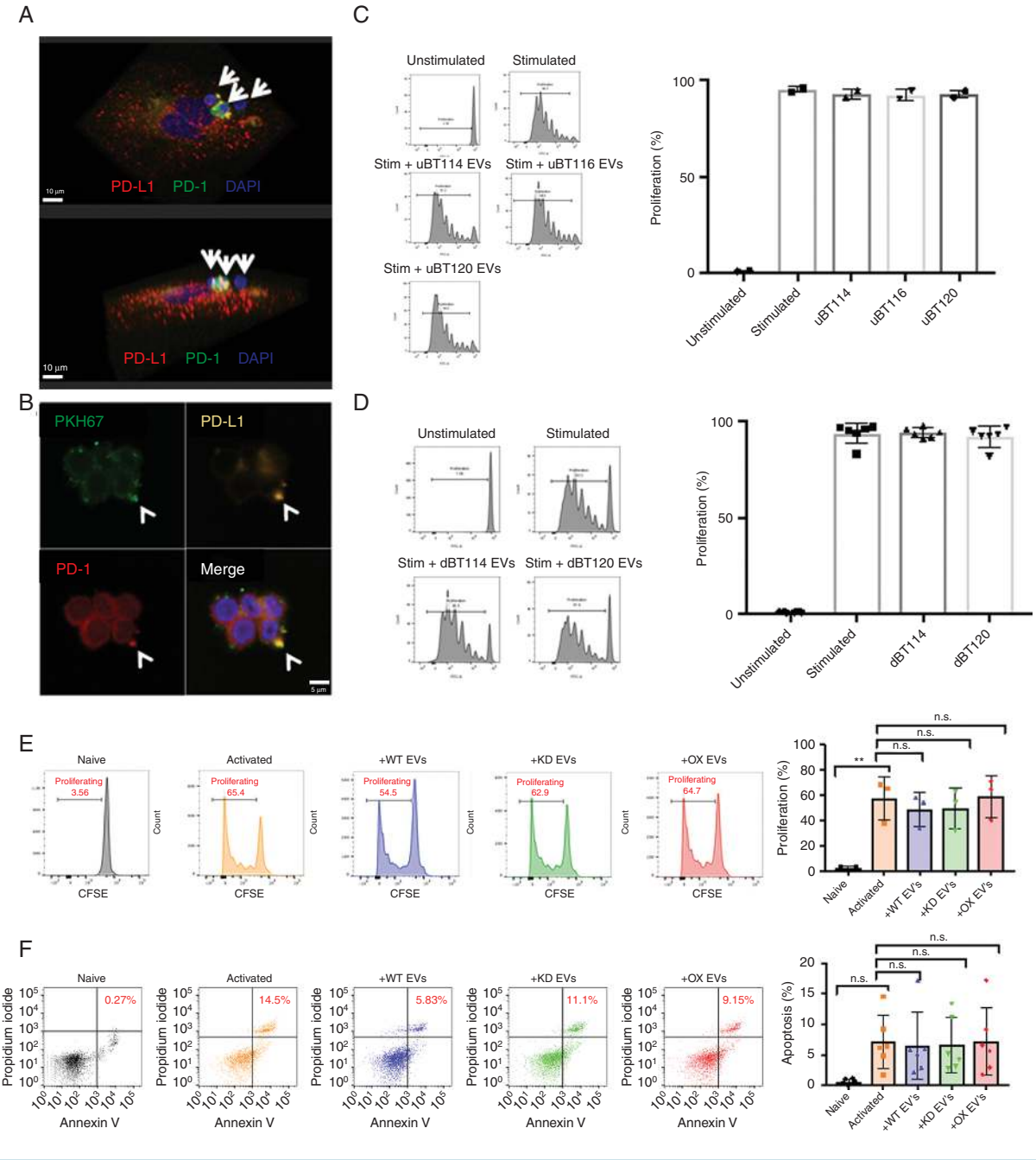

Fig. 2 Direct T-cell inhibition by glioblastoma EVs is modest regardless of PD-L1 expression. (A, B) Confocal micrographs demonstrating EVs association with T cells along PD-1/PD-L1 interactions (A, scale bar 10 μm) and PD-1/PD-L1 interaction in addition to PKH67 membrane staining of EVs in their entirety (B, scale bar 5 μm) demonstrating PD-1/PD-L1 interactions colocalize to T-cell-EV sites of interaction. (C) T cells labeled with CFSE were stimulated with antiCD3/CD28 beads in the presence or absence of uBT EVs as indicated. Proliferation was assessed at 72 hours following activation. Representative flow cytometry histograms of CFSE dilution shown at left with quantification at right. (D) As in (C), but T cells co-cultured with dBT-derived EVs. (E) T cell proliferation experiments as previously described, using EVs derived from dBT116 WT, PD-L1 KD, or PD-L1 OX cell lines as indicated. Comparisons performed using repeated measures (matched) ANOVA. (F) Cell death assay via propidium iodide/annexin V staining in T cells treated with dBT116 EVs as in (E). Comparisons performed using repeated measures (matched) ANOVA.

of immunosuppressive monocytes following EV treatment. We found that EVs from all 3 cell lines induced MDSC formation, regardless of PD-L1 expression (17.4% of all cells in unconditioned monocytes vs 42.4% in WT, 57.7% in KD, and 44.5%, $P = 0.005$, <0.0001, and 0.0024, respectively; Fig. 5A). However, EVs derived from dBT116 cells overexpressing PD-L1 induced the formation of more NCMs than EVs from either WT or PD-L1 KD cell lines (15.4% of cells vs 1.4% in

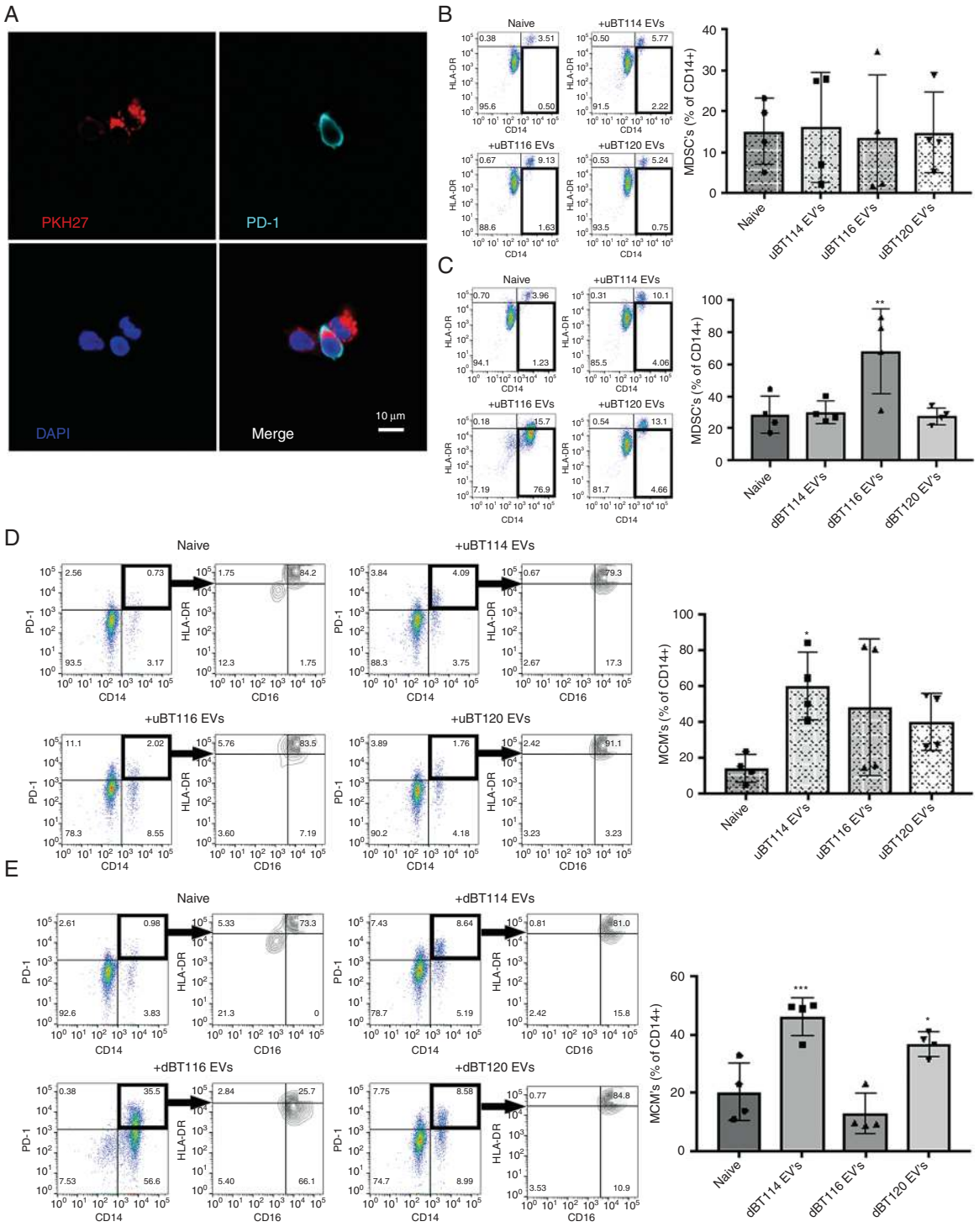

Fig. 3 Glioblastoma EVs induce myeloid-derived suppressor cells and nonclassical monocytes. (A) EVs (PKH27 stained, red) colocalize with PD-1 staining (white) upon co-culture with monocytes (scale bar 10 µm). (B) Co-culture of uBT-derived EVs and monocytes with staining for myeloid-derived suppressor cells (CD14+/HLA-Dr^{low}). No difference in MDSC formation was observed relative to naïve cells. Bar graphs presented as a percentage of CD14+ cells. (C) Induction of MDSCs by co-culture of monocytes with dBT-derived EVs. Comparisons performed using one-way ANOVA **, adjusted $P \leq 0.01$, Dunnett correction for multiple comparisons with naïve monocytes as reference group. (D) Induction of non-classical monocytes (CD14+/CD11b+/CD16+/HLA-DR^{high}) upon co-culture with uBT-derived EVs. Comparisons performed using one-way ANOVA *adjusted $P < 0.05$, correction for multiple comparisons. (E) Induction of nonclassical monocytes upon co-culture of monocytes with dBT derived EVs. Comparisons using one-way ANOVA ***adjusted $P \leq 0.001$, Dunnett correction for multiple comparisons.

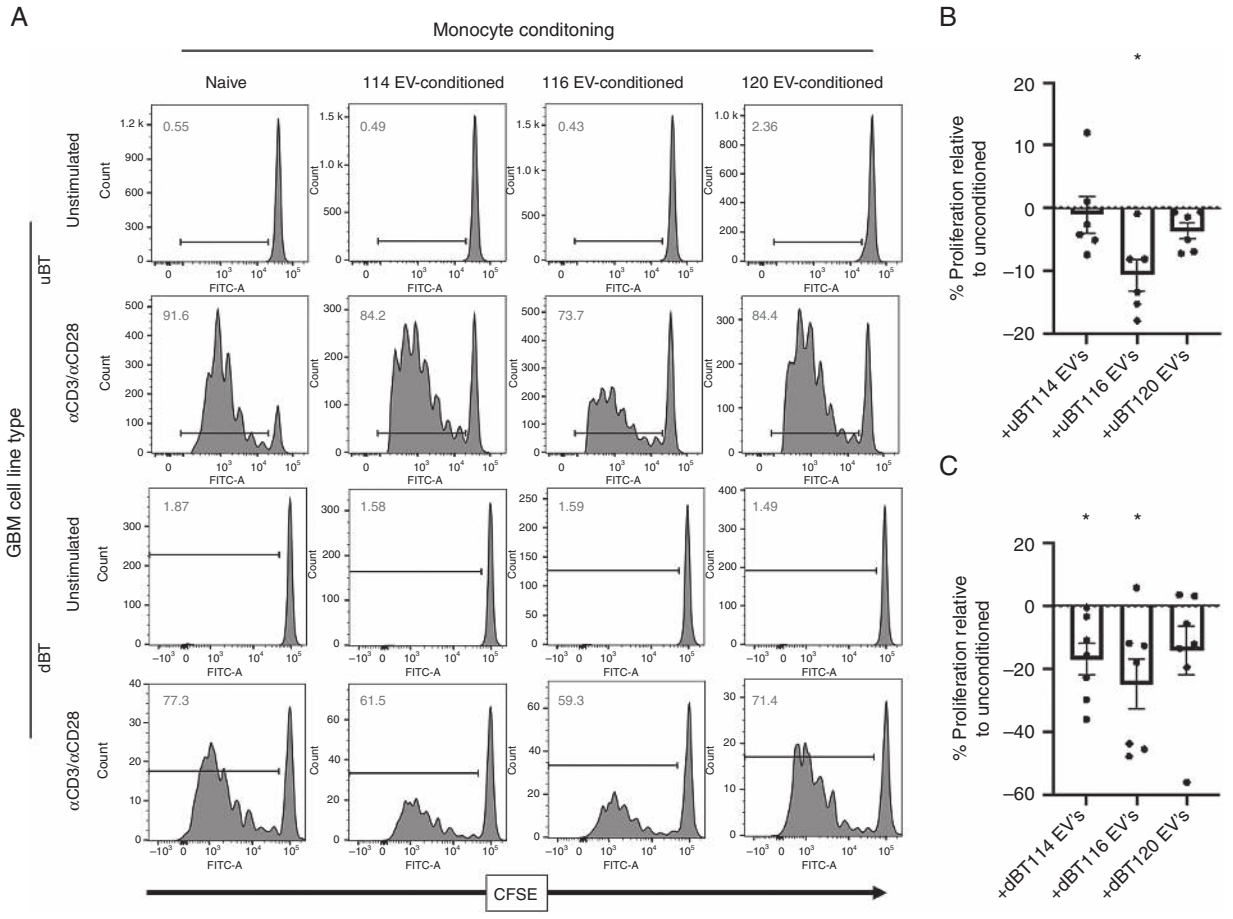

Fig. 4 Glioblastoma EV induced myeloid-derived suppressor cells and non-classical monocytes are immunosuppressive. (A) Following conditioning with either uBT-derived (top row) or dBT-derived (bottom row) EVs, monocytes were co-cultured with donor-matched CFSE-labeled T cells. T cells were activated with antiCD3/antiCD28 beads and co-cultured with monocytes for 5 days. Percentage proliferation in red for the representative sample displayed. (B) Percentages of T cells with reduced CFSE as described in A for uBT co-culture experiments ($n = 6$). Repeated measures ANOVA *adjusted $P < 0.05$, Dunnett correction for multiple comparisons. (C) Percentage of $CFSE^{low}$ T cells from dBT co-culture experiments described ($n = 7$). Repeated measures ANOVA *adjusted $P < 0.05$ Dunnett correction for multiple comparisons.

conditioned monocytes, $P = 0.0017$; Fig. 5B). Lastly, we sought to examine the overall immunosuppressive effect of monocytes treated with GBM-EVs with altered PD-L1 expression. Monocytes were co-cultured with EVs from dBT116 cell lines with normal, increased, or decreased PD-L1 expression and subsequently co-cultured with donor-matched CFSE-labeled T cells activated with αCD3/αCD28 stimulation. EVs from all 3 dBT116 cell lines significantly inhibited T-cell proliferation compared with co-culture with untreated monocytes or T cells alone, but this was not dependent upon PD-L1 expression (Fig. 5C).

Discussion

Immunosuppression in GBM remains a major obstacle to effective immunotherapy. Here we describe a potential mechanism for GBM-mediated immunosuppression—the induction of immunosuppressive monocytes by tumor-derived EVs. These suppressive cells have the potential to exert immunosuppressive effects both locally and systemically through the release of immunosuppressive cytokines such as IL-10. Unlike recent findings from Ricklefs et al,[6] we do not see evidence of direct T-cell inhibition by GBM-EVs. This may reflect different T-cell stimulation strategies (CD3 stimulation alone vs CD3/CD28 stimulation). While we believe the method used here represents a more physiologic activation of T cells than CD3 stimulation alone, it is possible that this stronger stimulation may mask a subtle direct inhibitory effect due to either EVs or PD-L1 that we were unable to observe.

The precise role of immunosuppressive monocytes in cancer remains an active area of investigation. There is increasing evidence that MDSCs are a heterogeneous population, and may represent only one of a number of immunosuppressive monocyte populations induced by cancer.[41,42] PD-1+ nonclassical monocytes as discussed

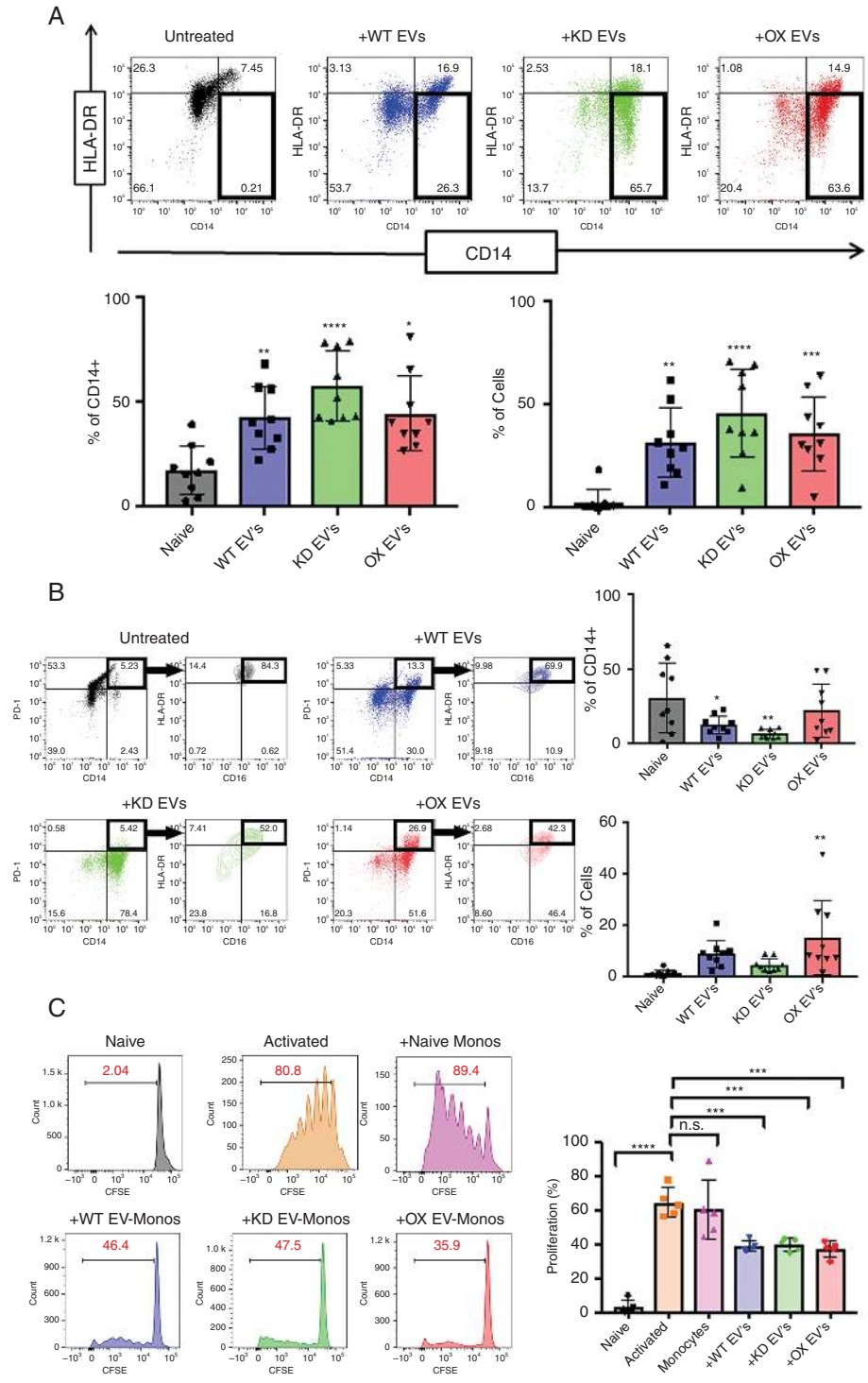

Fig. 5 Nonclassical monocyte but not myeloid-suppressor cell induction by glioblastoma EV's requires PD-L1. (A) Top: gating strategy for CD14+HLA-DR^{low} MDSCs derived from monocytes co-cultured with EVs derived from wild type (WT), PD-L1 shRNA knockdown (KD), or PD-L1 overexpressing (OX) dBT116 glioblastoma cells. Bottom: percentage of CD14+ (left) and total (right) cells of MDSCs derived from co-culture with the indicated EVs ($n = 9$ per group), comparison by one-way ANOVA **, adjusted $P \leq 0.01$,***, adjusted $P \leq 0.001$ ****, adjusted $P < 0.0001$, Dunnett correction for multiple comparisons. (B) Left: gating strategy for CD14+PD-1+CD16+HLA-DR^{high} non-classical monocytes derived from co-cultured with dBT116 EVs as in A. Right: percentage of CD14+ (top) and total (bottom) cells of NCMs derived from co-culture with the indicated EVs ($n = 9$ per group). Comparison by one-way ANOVA *, adjusted $P < 0.05$, **, ≤0.01, Dunnett correction for multiple comparisons. (C) Left: T-cell proliferation following anti-CD3/anti-CD28 activation measured by CFSE labeling following co-cultured with donor-matched monocytes conditioned with the indicated EVs. Right: quantification of T-cell proliferation, $n = 5$ per group. Comparisons by repeated measures (matched) ANOVA, ***adjusted $P < 0.001$, ****adjusted $P < 0.0001$, Dunnett correction for multiple comparisons.

here represent another such immunosuppressive cell type.[22,39,43] Our demonstration that PD-1+ NCMs are induced by EVs from multiple GBM cell lines in a PD-L1–dependent fashion, coupled with our findings that these cells are present in the tumor microenvironment of freshly resected GBM, point to NCMs as a significant contributor to GBM-mediated immunosuppression.

Ultimately, EVs are a heterogeneous population, exerting multiple modulatory effects on target cells. Strategies to isolate specific types of EVs are evolving, including the use of nanoscale flow cytometry, but such technologies are still in relative infancy, making it difficult to ascribe specific functions to specific subsets of EVs. Further, the functionality of EVs may vary from tumor to tumor, as evidenced in our study by the preferential induction of MDSCs by dBT116 EVs and NCMs by dBT114 and dBT120 EVs. This divergence of effect points to likely diversity of EV cargo, with tumors employing multiple EV-mediated immune evasion strategies. Increased signal transducer and activator of transcription 3 expression in GBM has been shown to have immunosuppressive effects in the tumor microenvironment, affect human leukocyte antigen D related expression, and be carried in EVs, suggesting a possible role in this process that merits further investigation.[44–46]

Our findings that MDSCs are readily induced by conditioning with EVs from some but not all GBM cell lines and that this induction is PD-L1 independent underscores the need to develop further understanding of the intricacies of EV-based signaling. EVs are functionally complex, carrying both membrane-bound and cytosolic protein payloads as well as small RNAs that can modulate target cells. EVs can act through ligand binding on the cell surface, endocytotic uptake into the target cell, or direct membrane fusion, each of which has significant implications for downstream signaling in the target cell. Given the complexity of these interactions, and the multiplicity of mechanisms with which tumor-derived EVs may be able to exert immunosuppressive effects on host cells, inhibiting the release of EVs from tumor cells or inhibiting EV-target cell interactions may prove a fruitful strategy to prevent tumor-mediated immunosuppression in GBM.

Supplementary Material

Supplementary data are available at *Neuro-Oncology* online.

Keywords

extracellular vesicles | glioblastoma | immunosuppression

Funding

This study was supported by grants from the Brains Together for a Cure Foundation and the Neurosurgery Research and Education Foundation.

Conflict of interest statement. The authors have no conflicts of interest related to any of the materials contained in this study.

Authorship statement. BTH, TEP, MPG, ABD, AJJ, HD, RLM, SM, and IFP contributed to experimental design. TEP, JT, and MJ performed western blotting and immunofluorescence studies. TEP developed PDL1 knockout and overexpression cell lines. BTH, TEP, SU, DY, HJLL, MA, and DP performed all flow cytometry studies and harvested extracellular vesicles. RLM and SM contributed regulatory T cell experiments. BTH and IFP analyzed flow cytometry data. MLCG and FL performed nanoscale flow cytometry experiments and analysis. BTH wrote the manuscript with contributions to methods from TEP and LMCG. All authors critically revised and approved of the final manuscript.

References

1. Stupp R, Mason WP, van den Bent MJ, et al; European Organisation for Research and Treatment of Cancer Brain Tumor and Radiotherapy Groups; National Cancer Institute of Canada Clinical Trials Group. Radiotherapy plus concomitant and adjuvant temozolomide for glioblastoma. *N Engl J Med*. 2005;352(10):987–996.
2. Omuro A, DeAngelis LM. Glioblastoma and other malignant gliomas: a clinical review. *JAMA*. 2013;310(17):1842–1850.
3. Young RM, Jamshidi A, Davis G, Sherman JH. Current trends in the surgical management and treatment of adult glioblastoma. *Ann Transl Med*. 2015;3(9):121.
4. Lim M, Xia Y, Bettegowda C, Weller M. Current state of immunotherapy for glioblastoma. *Nat Rev Clin Oncol*. 2018;15(7):422–442.
5. Preusser M, Lim M, Hafler DA, Reardon DA, Sampson JH. Prospects of immune checkpoint modulators in the treatment of glioblastoma. *Nat Rev Neurol*. 2015;11(9):504–514.
6. Ricklefs FL, Alayo Q, Krenzlin H, et al. Immune evasion mediated by PD-L1 on glioblastoma-derived extracellular vesicles. *Sci Adv*. 2018;4(3):eaar2766.
7. Herbst RS, Soria JC, Kowanetz M, et al. Predictive correlates of response to the anti-PD-L1 antibody MPDL3280A in cancer patients. *Nature*. 2014;515(7528):563–567.
8. Herbst RS, Baas P, Kim DW, et al. Pembrolizumab versus docetaxel for previously treated, PD-L1-positive, advanced non-small-cell lung cancer (KEYNOTE-010): a randomised controlled trial. *Lancet*. 2016;387(10027):1540–1550.
9. Parsa AT, Waldron JS, Panner A, et al. Loss of tumor suppressor PTEN function increases B7-H1 expression and immunoresistance in glioma. *Nat Med*. 2007;13(1):84–88.
10. Parney IF. Basic concepts in glioma immunology. *Adv Exp Med Biol*. 2012;746:42–52.
11. Fecci PE, Mitchell DA, Whitesides JF, et al. Increased regulatory T-cell fraction amidst a diminished CD4 compartment explains cellular immune defects in patients with malignant glioma. *Cancer Res*. 2006;66(6):3294–3302.
12. Chongsathidkiet P, Jackson C, Koyama S, et al. Sequestration of T cells in bone marrow in the setting of glioblastoma and other intracranial tumors. *Nat Med*. 2018;24(9):1459–1468.

13. Gustafson MP, Lin Y, New KC, et al. Systemic immune suppression in glioblastoma: the interplay between CD14+HLA-DR$^{lo/neg}$ monocytes, tumor factors, and dexamethasone. *Neuro Oncol.* 2010;12(7):631–644.
14. Vuk-Pavlović S, Bulur PA, Lin Y, et al. Immunosuppressive CD14+HLA-DR$^{low/-}$ monocytes in prostate cancer. *Prostate.* 2010;70(4):443–455.
15. Lin Y, Gustafson MP, Bulur PA, Gastineau DA, Witzig TE, Dietz AB. Immunosuppressive CD14+HLA-DR(low)/- monocytes in B-cell non-Hodgkin lymphoma. *Blood.* 2011;117(3):872–881.
16. Rodrigues JC, Gonzalez GC, Zhang L, et al. Normal human monocytes exposed to glioma cells acquire myeloid-derived suppressor cell-like properties. *Neuro Oncol.* 2010;12(4):351–365.
17. Gustafson MP, Lin Y, Bleeker JS, et al. Intratumoral CD14+ cells and circulating CD14+HLA-DRlo/neg monocytes correlate with decreased survival in patients with clear cell renal cell carcinoma. *Clin Cancer Res.* 2015;21(18):4224–4233.
18. Ostrand-Rosenberg S. Myeloid derived-suppressor cells: their role in cancer and obesity. *Curr Opin Immunol.* 2018;51:68–75.
19. Kumar V, Patel S, Tcyganov E, Gabrilovich DI. The nature of myeloid-derived suppressor cells in the tumor microenvironment. *Trends Immunol.* 2016;37(3):208–220.
20. Mosser DM, Edwards JP. Exploring the full spectrum of macrophage activation. *Nat Rev Immunol.* 2008;8(12):958–969.
21. Qorraj M, Bruns H, Böttcher M, et al. The PD-1/PD-L1 axis contributes to immune metabolic dysfunctions of monocytes in chronic lymphocytic leukemia. *Leukemia.* 2017;31(2):470–478.
22. Said EA, Dupuy FP, Trautmann L, et al. Programmed death-1-induced interleukin-10 production by monocytes impairs CD4+ T cell activation during HIV infection. *Nat Med.* 2010;16(4):452–459.
23. Zasada M, Lenart M, Rutkowska-Zapała M, et al. Analysis of PD-1 expression in the monocyte subsets from non-septic and septic preterm neonates. *PLoS One.* 2017;12(10):e0186819.
24. Ka MB, Gondois-Rey F, Capo C, et al. Imbalance of circulating monocyte subsets and PD-1 dysregulation in Q fever endocarditis: the role of IL-10 in PD-1 modulation. *PLoS One.* 2014;9(9):e107533.
25. Goswami S, Basu S, Sharma P. A potential biomarker for anti-PD-1 immunotherapy. *Nat Med.* 2018;24(2):123–124.
26. Raposo G, Stoorvogel W. Extracellular vesicles: exosomes, microvesicles, and friends. *J Cell Biol.* 2013;200(4):373–383.
27. Tkach M, Théry C. Communication by extracellular vesicles: where we are and where we need to go. *Cell.* 2016;164(6):1226–1232.
28. D'Souza-Schorey C, Clancy JW. Tumor-derived microvesicles: shedding light on novel microenvironment modulators and prospective cancer biomarkers. *Genes Dev.* 2012;26(12):1287–1299.
29. Skog J, Würdinger T, van Rijn S, et al. Glioblastoma microvesicles transport RNA and proteins that promote tumour growth and provide diagnostic biomarkers. *Nat Cell Biol.* 2008;10(12):1470–1476.
30. Javeed N, Gustafson MP, Dutta SK, et al. Immunosuppressive CD14+HLA-DR$^{lo/neg}$ monocytes are elevated in pancreatic cancer and "primed" by tumor-derived exosomes. *Oncoimmunology.* 2017;6(1):e1252013.
31. Kelly JJ, Stechishin O, Chojnacki A, et al. Proliferation of human glioblastoma stem cells occurs independently of exogenous mitogens. *Stem Cells.* 2009;27(8):1722–1733.
32. Frigola X, Inman BA, Lohse CM, et al. Identification of a soluble form of B7-H1 that retains immunosuppressive activity and is associated with aggressive renal cell carcinoma. *Clin Cancer Res.* 2011;17(7):1915–1923.
33. Dietz AB, Bulur PA, Emery RL, et al. A novel source of viable peripheral blood mononuclear cells from leukoreduction system chambers. *Transfusion.* 2006;46(12):2083–2089.
34. Gomes J, Lucien F, Cooper TT, et al. Analytical considerations in nanoscale flow cytometry of extracellular vesicles to achieve data linearity. *Thromb Haemost.* 2018;118(9):1612–1624.
35. Han SJ, Ahn BJ, Waldron JS, et al. Gamma interferon-mediated superinduction of B7-H1 in PTEN-deficient glioblastoma: a paradoxical mechanism of immune evasion. *Neuroreport.* 2009;20(18):1597–1602.
36. Kumar R, de Mooij T, Peterson TE, et al. Modulating glioma-mediated myeloid-derived suppressor cell development with sulforaphane. *PLoS One.* 2017;12(6):e0179012.
37. Noman MZ, Desantis G, Janji B, et al. PD-L1 is a novel direct target of HIF-1α, and its blockade under hypoxia enhanced MDSC-mediated T cell activation. *J Exp Med.* 2014;211(5):781–790.
38. Ohl K, Tenbrock K. Reactive oxygen species as regulators of MDSC-mediated immune suppression. *Front Immunol.* 2018;9:2499.
39. Gordon SR, Maute RL, Dulken BW, et al. PD-1 expression by tumour-associated macrophages inhibits phagocytosis and tumour immunity. *Nature.* 2017;545(7655):495–499.
40. Ziegler-Heitbrock L, Hofer TP. Toward a refined definition of monocyte subsets. *Front Immunol.* 2013;4:23.
41. Bronte V, Brandau S, Chen SH, et al. Recommendations for myeloid-derived suppressor cell nomenclature and characterization standards. *Nat Commun.* 2016;7:12150.
42. Tcyganov E, Mastio J, Chen E, Gabrilovich DI. Plasticity of myeloid-derived suppressor cells in cancer. *Curr Opin Immunol.* 2018;51:76–82.
43. Biswas SK, Mantovani A. Macrophage plasticity and interaction with lymphocyte subsets: cancer as a paradigm. *Nat Immunol.* 2010;11(10):889–896.
44. See AP, Han JE, Phallen J, et al. The role of STAT3 activation in modulating the immune microenvironment of GBM. *J Neurooncol.* 2012;110(3):359–368.
45. Poschke I, Mougiakakos D, Hansson J, Masucci GV, Kiessling R. Immature immunosuppressive CD14+HLA-DR$^{-/low}$ cells in melanoma patients are Stat3^{hi} and overexpress CD80, CD83, and DC-sign. *Cancer Res.* 2010;70(11):4335–4345.
46. Liu Y, Luo F, Wang B, et al. STAT3-regulated exosomal miR-21 promotes angiogenesis and is involved in neoplastic processes of transformed human bronchial epithelial cells. *Cancer Lett.* 2016;370(1):125–135.